

EXHIBIT P

Materials characterization and histological analysis of explanted polypropylene, PTFE, and PET hernia meshes from an individual patient

A. J. Wood · M. J. Cozad · D. A. Grant ·
A. M. Ostdiek · S. L. Bachman · S. A. Grant

Received: 19 September 2012 / Accepted: 18 January 2013 / Published online: 31 January 2013
© Springer Science+Business Media New York 2013

Abstract During its tenure in vivo, synthetic mesh materials are exposed to foreign body responses, which can alter physicochemical properties of the material. Three different synthetic meshes comprised of polypropylene, expanded polytetrafluoroethylene (ePTFE), and polyethylene terephthalate (PET) materials were explanted from a single patient providing an opportunity to compare physicochemical changes between three different mesh materials in the same host. Results from infrared spectroscopy demonstrated significant oxidation in polypropylene mesh while ePTFE and PET showed slight chemical changes that may be caused by adherent scar tissue. Differential scanning calorimetry results showed a significant decrease in the heat of enthalpy and melt temperature in the polypropylene mesh while the ePTFE and PET showed little change. The presence of giant cells and plasma cells surrounding the ePTFE and PET were indicative of an active foreign body response. Scanning electron micrographs and

photo micrographs displayed tissue entrapment and distortion of all three mesh materials.

Keywords Polypropylene · ePTFE · PET · FT-IR · DSC · Histology

1 Introduction

Abdominal wall hernias are a significant concern in the United States, with an estimated 800,000 new cases every year, which amounts to one new case every minute [1]. This number will likely increase as obesity ($BMI \geq 30$) continues to rise in the United States. In 2008 the obesity prevalence for men was 32.2 and 35.5 % for women overall, while the prevalence of obesity in the U.S. grew approximately 5 % in all age categories for men and

A. J. Wood
Department of Biological Engineering, University
of Missouri-Columbia, 162 Agricultural Engineering Building,
Columbia, MO, USA
e-mail: Ajwq48@mail.missouri.edu

M. J. Cozad · A. M. Ostdiek
Department of Biological Engineering, University
of Missouri-Columbia, Room 148 Agricultural
Engineering Building, Columbia, MO 65211, USA
e-mail: mjcozad@mail.missouri.edu

A. M. Ostdiek
e-mail: ostdieka@mail.missouri.edu

D. A. Grant
Department of Biological Engineering, University
of Missouri-Columbia, Room 210 Agricultural
Engineering Building, Columbia, MO 65211, USA
e-mail: grantdav@mail.missouri.edu

S. L. Bachman
Department of General Surgery, University
of Missouri-Columbia, Mc423 McHaney Hall,
Columbia, MO 65211, USA
e-mail: bachmans@health.missouri.edu

S. A. Grant (✉)
Department of Biological Engineering, University
of Missouri-Columbia, Room 250 Agricultural
Engineering Building, Columbia, MO 65211, USA
e-mail: grantsa@missouri.edu

approximately 2–3 % in all age categories for women from 1999 to 2008 [2].

Since the mid-nineties, the most common method of repairing abdominal hernias has been the “tension-free” repair using a variety of synthetic mesh such as polyethylene, heavy weight polypropylene, expanded polytetrafluoroethylene (ePTFE), polyethylene terephthalate (PET), lightweight polypropylene, and even resorbable mesh materials [3]. But despite being a very common surgery, there is still a high percentage of primary hernia recurrence with the tension-free repair (10.1 % laparoscopic and 4 % open repair) and recurrent hernia repair (10.0 % laparoscopic and 14.1 % open repair) [4]. A large subset of recurrence surgeries may be due to the lack of mesh inertness *in vivo*. These materials result in a large foreign body response that some thought was necessary to repair the defect [3]. In recent years, there has been new evidence that a large foreign body response can result in physico-chemical changes in the mesh material, which may lead to poor patient outcomes and recurrences [5–7].

While synthetic mesh is frequently utilized to repair hernias, these materials are also being utilized as pelvic slings for urogynecologic applications. Unfortunately, these mesh materials, also composed of polypropylene, PET, and ePTFE, are experiencing biocompatibility problems which are resulting in groin pain and prolapse [8, 9]. On July 13, 2011, the FDA issued a statement warning surgeons and patients about the complications associated with surgical mesh. More recently, the FDA is considering reclassifying urogynecologic surgical mesh used to repair pelvic organ prolapsed from Class II to Class III [10].

Synthetic meshes are recognized as foreign bodies and thus, are subjected to various enzymatic attacks by the body. The primary attack on the material is from neutrophils and macrophages, which are stimulated upon injury or implantation. The cells release lysosomal enzymes and oxidants that can actively break down some of the mesh materials [11]. The resulting degradation inflicted on the mesh and the resulting effect on the patient is a subject which requires more investigation in order to understand the mesh material-patient interactions and ultimately improve future mesh-material designs. However a difficulty faced in these studies are the individual patient responses (or subset population responses). A variety of patient factors, such as BMI and diabetes, can influence the wound healing response in patients. This diversity in patient populations makes it difficult to draw conclusions on the mechanism of mesh degradation and thus makes it difficult to predict the overall effectiveness of a mesh material in patient populations. In this paper, we present a materials study where a single patient received three different hernia mesh materials: ePTFE, PET, and heavy weight polypropylene. The study provides insight on how

three different materials reacted in the same biological environment. By understanding the materials-tissue responses in subset populations, the guesswork of material selection can be reduced and better patient outcomes will be achieved.

2 Materials and methods

2.1 Explanted hernia meshes

The patient was a 55-year-old white male who presented to the surgical clinic in June of 1974 with the chief complaint of a ventral hernia and obstruction. The patient came to the hospital after experiencing severe pain at the hernia site. His medical history was positive for gout, morbid obesity (BMI = 37.4), and sleep apnea. A previous user of tobacco products, the patient’s surgical history also included a cholecystectomy. The patient had a total of three recurrent ventral hernia repairs. The dates for each surgery were June 2006, June 2007, and June 2009. Polypropylene and PET meshes were implanted in the June 2006 surgery. ePTFE was implanted in the June 2007 surgery. Three meshes of different materials (polypropylene, ePTFE, and PET) were explanted on the third recurrent hernia repair surgery in June 2009. The hernia meshes were removed due to ventral hernia recurrence and pain.

The hernia mesh specimens were removed from the patient according to an approved IRB protocol. Implantation time for the meshes were 3 years for the polypropylene and PET meshes and 2 years for the ePTFE mesh. Pristine samples of polypropylene, PET, and ePTFE meshes were utilized as a control comparison to the explants.

Upon removal from the patient, the explants were placed in a 10 % v/v formalin solution at room temperature. This was followed by a 2 h immersion in sodium hypochlorite (13 % active chlorine, Acros Organics, Morris Plains, NJ) to remove residual tissue from the mesh. Distilled water was then used to remove the sodium hypochlorite solution through a series of four rinses. Pristine samples were also subjected to this cleaning protocol before characterization. Our previous, unpublished studies show that the cleaning process does not induce any damage to the pristine mesh materials nor the explanted mesh.

2.2 Digital images

After cleaning, digital images were taken of the explants. Figure 1 shows an example of each pristine mesh and the corresponding explanted meshes. The pristine meshes are shown at a higher magnification so that the structure/porosity of the mesh can be observed. The explanted meshes are shown at a lower magnification so that

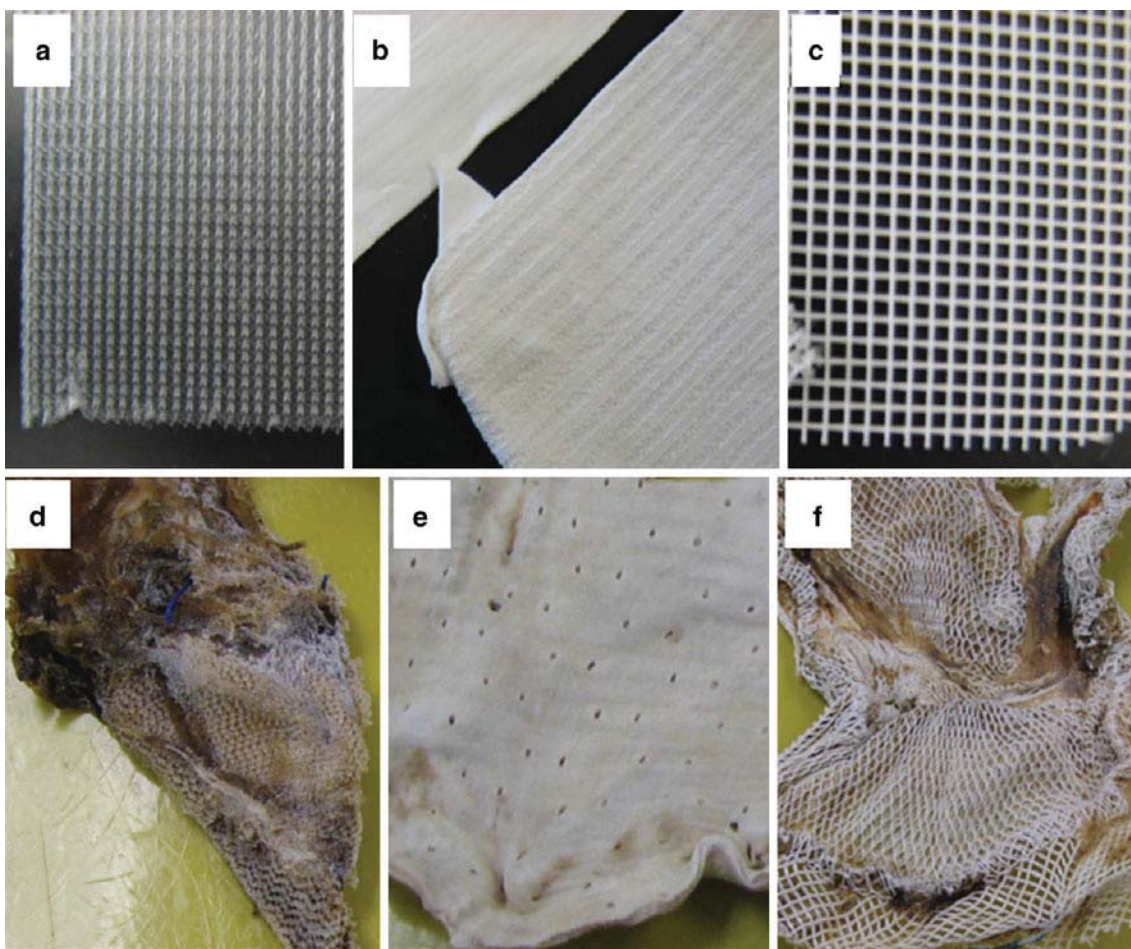


Fig. 1 Pristine samples of **a** polypropylene, **b** ePTFE, and **c** PET hernia mesh. Samples of explanted **d** polypropylene, **e** ePTFE, and **f** PET hernia mesh

discoloration and distortion of the mesh can be observed. In some locations on the explanted mesh, the distortion is permanent.

2.3 Scanning electron microscopy (SEM)

SEM was conducted to visually observe the surface morphology. Uncoated material samples from the hernia mesh explants and pristine specimens were viewed using a Quanta 600F Environmental SEM (FEI Company, Hillsboro, OR). Secondary electron images were taken using an accelerating voltage of 10 kV, 0.38 torr chamber pressure, and a 10–11.3 mm working distance.

2.4 Attenuated total reflectance fourier transform infrared spectroscopy (ATR-FTIR)

ATR-FTIR uses the absorption of infrared light due to the vibration characteristics of different bonds to identify chemical functional groups in a sample. Utilizing the ATR-FTIR, the specimens were analyzed to determine if any

surface chemical changes (absence or presence of functional groups) occurred during their *in vivo* tenure. The ATR crystal was utilized in order to perform surface scans which have a penetration depth of 2–4 μ m. Spectra of polypropylene, PET, and ePTFE samples ($n = 6$) and corresponding pristine samples ($n = 6$) were collected by averaging 32 scans completed by a Nicolet 6700 FTIR spectrometer (Thermo Scientific, Waltham, MA) with a 4 cm^{-1} resolution at ambient temperature. To determine if oxidation occurred in the polypropylene mesh, a quantitative comparison between samples and pristine was performed by integrating the carbonyl peak at 1,740 cm^{-1} from the ATR-FTIR spectrum over the range 1,780–1,690 cm^{-1} . For ePTFE, $\text{CF}=\text{CF}/\text{C}=\text{O}$ peaks were integrated over the range 1,770–1,690 cm^{-1} , and for ePTFE, the change in the 1,720 cm^{-1} $\text{C}=\text{O}$ over the range 1,790–1,650 cm^{-1} was examined. Additionally, integration was also performed on the peaks at 1,450 and 1,339 cm^{-1} for ePTFE and PET to determine the formation of additional surface hydrocarbons [12]. The first ePTFE peak at 1,450 cm^{-1} was integrated between 1,490 and 1,430 cm^{-1} .

The second ePTFE peak at $1,339\text{ cm}^{-1}$ was integrated between $1,390$ and $1,330\text{ cm}^{-1}$. The first PET peak at $1,450\text{ cm}^{-1}$ was integrated between $1,490$ and $1,420\text{ cm}^{-1}$. The second PET peak at $1,339\text{ cm}^{-1}$ was integrated between $1,350$ and $1,310\text{ cm}^{-1}$.

The 1740 , 1450 , and $1,339\text{ cm}^{-1}$ peak areas from each mesh were divided by a reference peak area located at $2,720\text{ cm}^{-1}$ for polypropylene, 2366 cm^{-1} for ePTFE, and $1,410\text{ cm}^{-1}$ for PET. This was performed to normalize the peak areas and obtain peak indices. The indexed peak areas for the pristine and explanted samples were compared using GraphPad Prism v4.0 (GraphPad Software, San Diego, CA) to obtain percent differences between the means. To eliminate any pressure positioning errors with the ATR crystal, six measurements were taken and averaged for each specimen. The specimen holder on the ATR-FTIR applies consistent pressure, thus reducing errors.

2.5 Modulated differential scanning calorimetry (MDSC)

MDSC provides thermochemical data of bulk materials and thus can be used to determine a wide range of physical properties of materials, such as the heat of enthalpy (ΔH) and the melting temperature T_m . Heat of enthalpy is defined as heat flow (energy) into a system which alters the materials molecular structure while the melt temperature is defined as the temperature at which the rigid structure of the molecules breaks down into a less ordered state. There is a phase change from solid to liquid. Samples ($n = 3$) from all three mesh types (PP, PET, and ePTFE) and corresponding pristine samples ($n = 3$) were prepared for MDSC to create thermal stability profiles. Samples ($5 \times 5\text{ mm}$) were obtained from the most “pristine-like” locations on the meshes to avoid the possibility of microscopic tissue adhesion. The samples were then hermetically-sealed in aluminum pans and subjected to MDSC under nitrogen flow using a Q2000 DSC (TA Instruments, New Castle, DE). Testing parameters included a ramp rate of $3\text{ }^{\circ}\text{C min}^{-1}$, a modulation of $\pm 64\text{ }^{\circ}\text{C}$ every 80 s , an initial temperature of $-90\text{ }^{\circ}\text{C}$, and a final temperature of 220 , 300 , and $425\text{ }^{\circ}\text{C}$ for PP, PET, and ePTFE, respectively. Results were returned in the form of thermograms with a plot of total heat flow (W/g) versus temperature ($^{\circ}\text{C}$) from which ΔH and T_m were determined.

2.6 Histology

Histological analysis was performed on representative samples from the ePTFE and PET meshes. Polypropylene mesh was not discovered in the patient explants until after the cleaning process, thus rendering the PP mesh ineligible for histology. The inability to detect polypropylene before

the cleaning process can be attributed to a large amount of fatty and scar tissue encompassing the meshes. Samples of the ePTFE and PET meshes were fixed in 10 \% formalin. They were embedded in paraffin, cut in $5\text{ }\mu\text{m}$ -thick sections, and processed for staining with hematoxylin and eosin (H&E). Viewing was done on a Zeiss Axiohot (Carl Zeiss Microimaging, Inc., Thornwood, NY) and photographs were taken using an Olympus DP70 (Olympus America Inc., Center Valley, PA) camera with DP Manager Version 1.21.107 as the acquisition software. Initially the slides were viewed at $10\times$ and $20\times$ to obtain an overall sense of the tissue reaction. Reactive areas were then examined and photographed at a magnification of $40\times$.

2.7 Statistical analyses

Experimental data was analyzed using GraphPad Prism v4.0 (GraphPad Software, San Diego, CA). One-way analysis of variance with a 95 \% confidence interval was conducted. This was followed by a Dunnett’s multiple comparison post-test to determine significant differences between the mean of the pristine group and the means of each of the experimental groups.

3 Results

3.1 SEM

SEM micrographs can be seen in Fig. 2. Micrographs of the pristine polypropylene mesh displayed relatively smooth surfaces with signs of extrusion while explanted polypropylene showed significant crazing/surface cracking which is indicative of oxidation [13]. ePTFE did not show any signs of surface degradation, but did show some shrinkage and tissue entrapment. The average pore size in the pristine sample (Fig. 2b) was measured to be between 150 and $200\text{ }\mu\text{m}$ while the explant (Fig. 2e) had significantly smaller pore sizes at 20 – $50\text{ }\mu\text{m}$. PET fibers did not show any morphological alteration in vivo; the fibers were still intact without any crazing or cracking.

3.2 ATR-FTIR

Figure 3 shows a representative spectrum collected from the explanted polypropylene mesh along with a spectrum of a pristine polypropylene mesh. The scans revealed a large peak at $\sim 1,740\text{ cm}^{-1}$, indicative of carbonyl groups (C=O), that was not evident in the pristine sample. This correlates with free radical formation and oxidation of the polypropylene mesh while in vivo [14–16]. The indexed area under the carbonyl peak for the explant was statistically higher ($p < 0.05$) than the pristine sample.

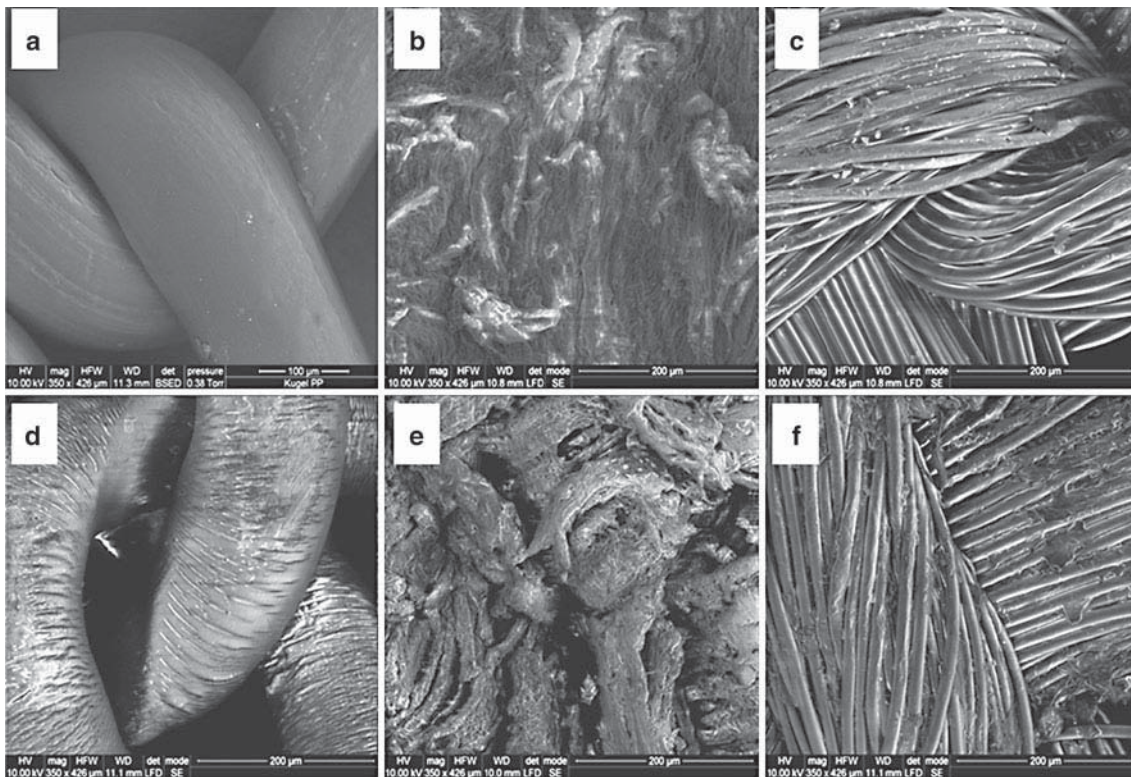


Fig. 2 SEM images of pristine **a** polypropylene, **b** ePTFE, and **c** PET hernia mesh as well as explanted **d** polypropylene, **e** ePTFE, and **f** PET hernia mesh

Fig. 3 ATR-FTIR scans of pristine polypropylene and a representative polypropylene explant illustrating the carbonyl (C=O) peak

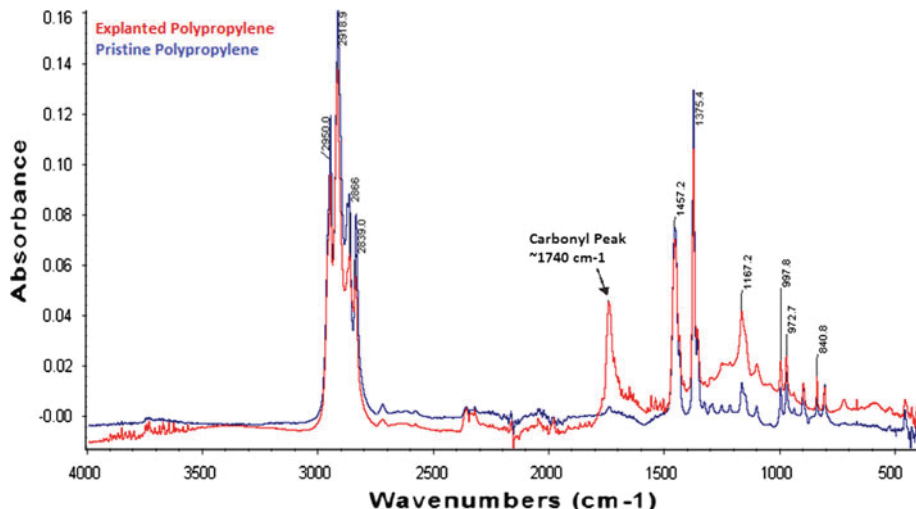


Figure 4 shows a representative spectrum collected from the explanted ePTFE mesh along with a spectrum of a pristine ePTFE mesh. The results of the scan showed the presence of a peak at $\sim 1,740 \text{ cm}^{-1}$ that was not present in the pristine ePTFE samples. This peak could represent $\text{CF}=\text{CF}$ bonds or a carbonyl group [17, 18]. Additionally, the explanted ePTFE samples demonstrated peaks at $\sim 1,450$ and $\sim 1,339 \text{ cm}^{-1}$, indicative of surface hydrocarbon formation, which could indicate the presence of scar

tissue and/or chemical degradation [12]. The area under each peak was measured and compared to the pristine ePTFE samples. It was found that the indexed area under the $\sim 1,740 \text{ cm}^{-1}$ peak was statistically higher ($p < 0.05$) than the pristine samples. The indexed area under the $\sim 1,450$ and $\sim 1,339 \text{ cm}^{-1}$ peaks were also statistically higher ($p < 0.05$) than the pristine samples.

Figure 5 shows a representative spectrum collected from the explanted PET mesh along with a spectrum of a pristine

Fig. 4 ATR-FTIR scans of pristine ePTFE and a representative ePTFE explant illustrating the carbonyl (C=O) peak and two C–H stretching peaks

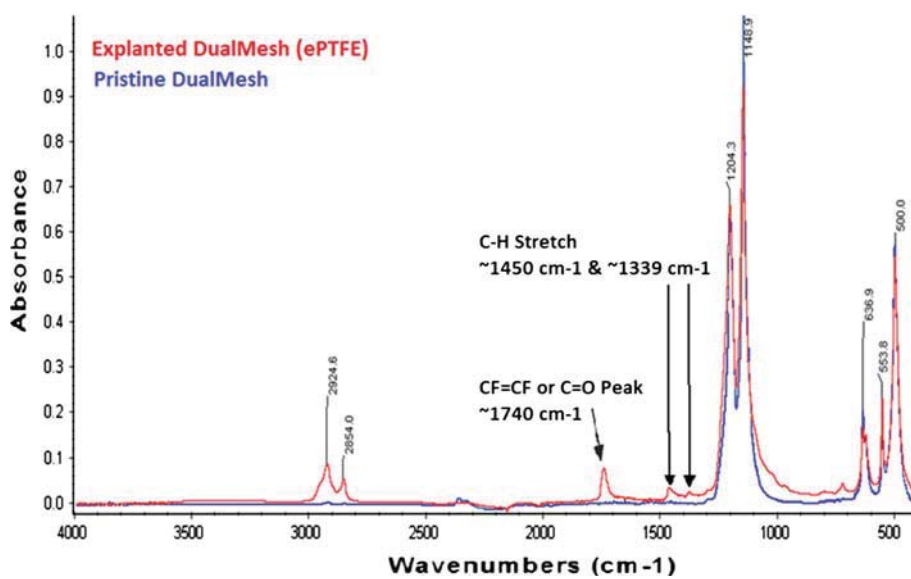
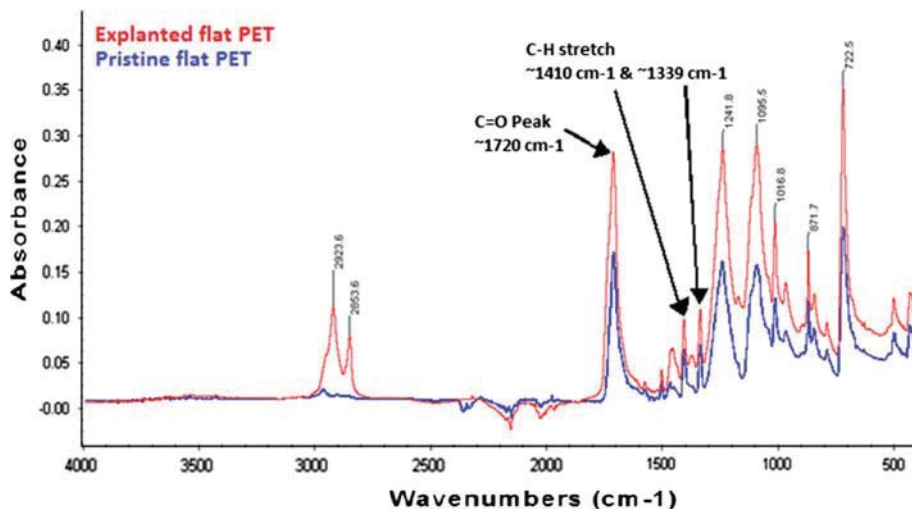


Fig. 5 ATR-FTIR scans of pristine PET and a representative PET explant illustrating the carbonyl (C=O) peak and two C–H stretching peaks



PET mesh. The scans revealed peaks in the explant spectrum at ~ 1720 , ~ 1410 , and $1,339\text{ cm}^{-1}$ that were larger than the peaks in the pristine sample scans. The peak at $\sim 1,720\text{ cm}^{-1}$ in the pristine sample is primarily caused by terephthalic esters present in the PET backbone [14]. The increased peak area in the explant samples at $\sim 1,720\text{ cm}^{-1}$ can be attributed to oxidation/hydrolysis in the form of carbonyl bonds and/or scar tissue trapped in the PET fibers that was not removed in the cleaning step. The indexed peak area at $\sim 1,720\text{ cm}^{-1}$ was statistically higher ($p < 0.05$) than the pristine. The indexed peak area at the $\sim 1,410\text{ cm}^{-1}$ peak was statistically higher than the pristine ($p < 0.05$).

3.3 MDSC

Figure 6 shows the statistical results from the MDSC data for all pristine and explanted samples. Polypropylene demonstrated a 58 % decrease ($p < 0.05$) in the heat of

enthalpy and 3 % decrease ($p < 0.05$) in melt temperature as compared with pristine. There were no significant difference between the ePTFE explants and the pristine ePTFE samples or between the PET explants and the pristine PET samples.

3.4 Histology

H&E stained sections of ePTFE showed the host tissue had not penetrated the material, but there were several reactive areas clinging to the periphery of the ePTFE. Figure 7 shows the presence of Langhan's- type giant cells and lymphocytes next to the ePTFE (as denoted by the arrows). Langhans-type giant cells are large cells that are formed by the fusion of macrophages, resulting in an arcuate arrangement of nuclei. The lymphocytes are white blood cells that carry out the responsibilities of the immune system. There was a small pocket of neutrophils present in

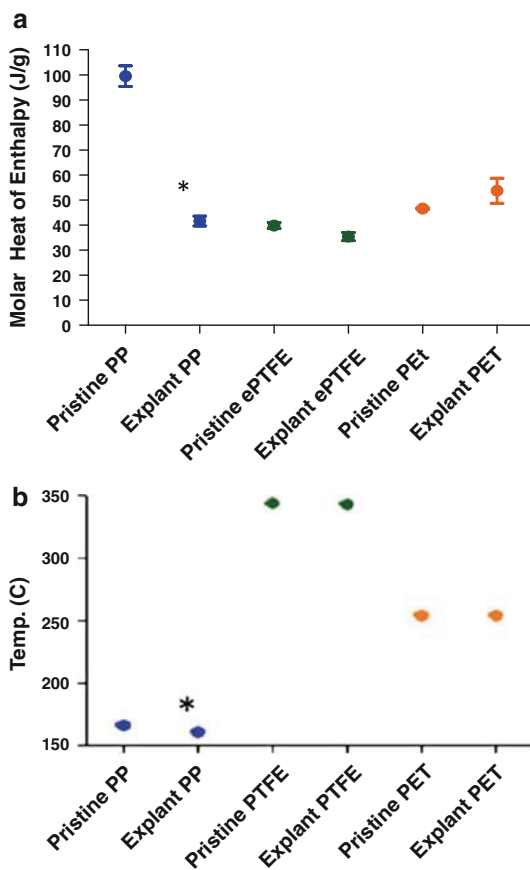


Fig. 6 MDSC results **a** heat of enthalpy, and **b** melt temperature for pristine and explanted polypropylene (PP), ePTFE, and PET samples. Statistical difference (* $p < 0.05$)

another view of the slide (not shown), but no signs of bacterial infection. Overall, the presents of these cells indicate a moderate granulomatous inflammatory reaction with occasional neutrophils, which is indicative of a chronic foreign body response. Figure 8 shows that PET is more integrated with the host tissue than ePTFE and has more fibrous tissue present. As denoted by the arrows, the PET is shown in the form of cylinders surrounded by tissue. There are signs of a chronic moderate granulomatous inflammatory reaction including several Langhans-type giant cells, lymphocytes, an occasional plasma cell and fibrous tissue interspersed with the PET fibers. Mild neovascularization was found to have taken place throughout the sections studied.

4 Discussion

A common factor demonstrated by all the explanted meshes was the permanent distortion of the mesh dimensions. As seen in Fig. 1d–f, the PP, ePTFE, and PET meshes have permanently deformed, either puckering at the

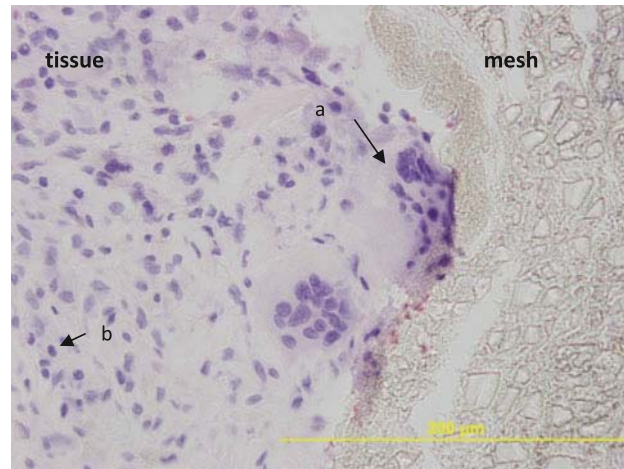


Fig. 7 Histology slide of ePTFE explants with H&E staining at 40 \times . The arrows are pointing at the Langhans-type giant cells, which are indicative of a continuous foreign body response (a) and at a lymphocyte (b)

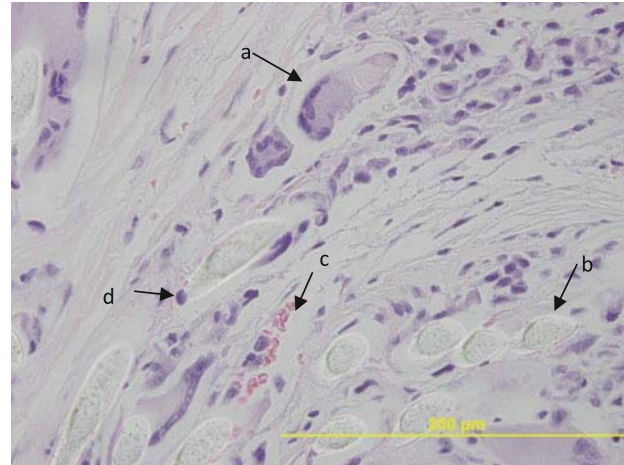


Fig. 8 Histology slide of PET explants with H&E staining at 40 \times . The mesh is shown as cylinders surrounded by tissue. The arrow is pointing at one of the Langhans-type giant cell (a), at one of the PET fibers (b), at the location of neovascularization (c), and one of the lymphocytes (d)

edges as in ePTFE or contracting and twisting with entwined tissue as with PP and PET. The cause for the distortion could be due to the inherent response of the body to foreign materials and the continual mechanical stresses encountered by the materials. During the foreign body response, scar tissue is deposited and fibrous encapsulation may occur. This can be compounded if there is continuous movement of the mesh due to normal physical activities of the patient. The laying down of myofibroblasts onto the mesh can result in contraction at the tissue-mesh interface resulting in the distortion of the mesh material and entrapment of tissue. In some cases, this tissue entrapment

is so dense that it is difficult to locate the mesh. Responses to the mesh such as these can result in recurrences. Additionally, enzymes and oxidants are also attacking the mesh which could result in chemical degradation of the mesh materials and thus permanent deformation. While the three different mesh materials showed similar visual responses with respect to distortion of mesh and tissue entrapment, they presented different mesh degradation responses.

4.1 Polypropylene

Polypropylene is a thermoplastic polymer; hence, it can be re-melted and reformed. Typically, polypropylene fibers are extruded in monofilament form and then woven into a particular monofilament or multi-filament design. With its methyl side groups off of the carbon backbone, polypropylene is hydrophobic, and it is usually resistant to many chemical solvents, bases and acids. Unfortunately, polypropylene will degrade in an oxidizing environment, such as the environment during a foreign body response. Because of this, polypropylene has been shown to oxidize *in vivo* [19]. Oxidation of polypropylene results in surface crazing and cracking, changes in mechanical strength, and increased brittleness. The SEM image shown in Fig. 2d demonstrates obvious crazing and cracking of the explanted polypropylene specimen as compared to the pristine mesh (Fig. 2a). Additionally, ATR-FTIR spectra in Fig. 3 confirmed the presence of carbonyl peaks which are indicative of surface oxidation. Previous studies have also shown the tendency of polypropylene to oxidize, which can be confirmed by the presence of the carbonyl peak [20].

Both the SEM and ATR-FTIR provide characterization of the surface morphology and surface chemistry, respectively, but it is also necessary to determine if the bulk properties of the polypropylene material also changes. Figure 6 displayed MDSC data which showed a significant difference in ΔH and T_m between the explant and the pristine samples. In both cases, the explanted samples displayed a lower heat of fusion and lower melt temperature. This is indicative of chemical changes within the bulk structure of the material. During thermo-mechanical stress, chain scission can occur in polypropylene [20]. Chain scission results in shortening of the polymer chains which results in decreased mechanical strength of the mesh that may lead to rupture and tearing of the mesh.

4.2 ePTFE

Expanded PTFE is one of the most chemically stable materials. With its carbon backbone and fluorine side chains, it is also a highly hydrophobic material. Its material inertness makes it difficult to chemically modify its surface and thus it is very resistant to enzymatic attack

by the foreign body response. However, ePTFE still has a less than ideal response when utilized as a hernia mesh. Literature has shown ePTFE to undergo significant shrinkage and distortion resulting in recurrences [21]. In Fig. 1e, the ePTFE sample also shows the characteristic distortion and discoloration. The microstructure of ePTFE provides an ideal environment for myofibroblast cells to reside and contract resulting in shrinkage and distortion of the mesh. The SEM micrograph in Fig. 2e confirms that some shrinkage occurs; however, very little if any degradation of the ePTFE is noted microscopically. Histology confirmed the presence of chronic phase inflammatory cells, such as the giant cells and lymphocytes with some acute phase neutrophils present. These results indicate the lack of long-term biocompatibility. FTIR results confirmed the presence of functional groups not present on the pristine. These groups can be indicative of some slight chemical changes, but most likely are due to the scar tissue entrapment within the microscopic structure of the ePTFE. Thermal data seems to confirm the results of the SEM. MDSC data displayed no significant difference between the explanted and pristine ePTFE samples in terms of melt temperature and heat of enthalpy, indicating that the bulk chemical structure of the ePTFE did not change *in vivo*.

4.3 PET

PET or better known as Dacron or polyester is processed in the form of a multi-filament fabric for hernia mesh materials as well as for other medical applications such as artificial vascular grafts. While still classified as hydrophobic, PET is more hydrophilic than PP. PET is susceptible to hydrolysis and has failed *in vivo* [22]. As a hernia mesh, PET also demonstrates scar tissue entrapment and distortion of the mesh as shown in Fig. 1f. Like ePTFE, PET did not display any morphological changes on the surface of the fibers as indicated in Fig. 2f. However, FTIR did demonstrate an increase C=O peak index over pristine, which is indicative of slight chemical modifications. The thermal data, MDSC, displayed no significant changes in the explanted PET compared to the pristine PET; however, the average heat of enthalpy and melt temperature were higher for the explants. These higher values can indicate that the material has undergone some type of crosslinking. Under mechanical stress, polyethylene will commonly undergo branching and chain crosslinking which changes the material properties [20]. As shown in the histology, the PET explants were integrated with the host tissue and showed more fibrous tissue formation and neovascularization. Like ePTFE, the mesh showed signs of chronic inflammation. These findings suggest the lack of long-term biocompatibility of synthetic materials.

All three mesh materials did not demonstrate tissue inertness. The mesh materials were distorted and/or contracted, along with tissue entrapment. The distortion appeared permanent in the PP mesh most likely due to changes in the materials properties caused by oxidation, while for the ePTFE and PET meshes, the distortion appears permanent as well but most likely due to scar tissue becoming entrapped within the mesh structure resulting in contraction. The continuous movement of the mesh during normal physical activities may have contributed to a continuous foreign body response, resulting in scar tissue. Mechanical stress and strain have been shown to affect the functionality of mesh materials [7, 23, 24]. Since all three mesh materials, PP, ePTFE, and PET, were implanted in a single patient, all three mesh experienced similar stresses on the abdominal wall that can be transferred to the mesh material. During the course of a normal day, the pressure within the abdomen can be elevated as during exercise or reduced as during periods of relaxation. This results in repetitive changes in stress and strain experienced by the mesh material. It is not conclusive whether this continuous loading and unloading results in reduced tensile strength or increase the strain of the mesh materials. However, a recent *in vitro* study demonstrated that the tensile strength of e-PTFE and polypropylene mesh was significantly reduced when undergoing continuous loading (1,000 cycles) while the strain increased [23]. These findings suggested that repetitive loading may lead to deterioration of the mechanical properties of the mesh material, which can lead to increase foreign body response and poor functional results.

5 Conclusion

Three different mesh materials were explanted from a single patient so that a side-by-side materials characterization could be performed. The polypropylene mesh demonstrated chemical degradation via oxidation, permanent distortion of the mesh, and changes in thermal properties. While chemical degradation was not conclusively evident in PET and ePTFE, the presence of scar tissue, the histology results, and contraction/distortion of the material were indicative of lack of long-term biocompatibility and lack of inertness. While the results of the characterization study showed that polypropylene will undergo oxidation, ePTFE and PET appeared to be more chemically resistant to the enzymatic attack from the foreign body response. However, this study showed that chemical resistance is not enough to ensure biocompatibility. Mesh distortion and scar formation were evident for all the materials. The next generation of mesh materials needs to promote new tissue regeneration and integration while avoiding scar tissue formation and fibrous encapsulation.

Acknowledgments This research was supported in part by the University of Missouri Life Sciences Predoctoral Fellowship, the University of Missouri F21C, and BICAM (Biomaterials Innovation, Characterization, and Analysis of Missouri) laboratory at the University of Missouri.

References

1. Everhart JE, editors. *Digestive diseases in the united states: epidemiology and impact*. Washington, DC: U.S. Government Printing Office 2004. National Institute of Health Publication No. 94-1447.
2. Flegal KM, Carroll M, Ogden C, Curtin L. Prevalence and trends in obesity among US adults: 1999–2008. *JAMA*. 2010;303(3): 235–1.
3. Iqbal Y. Controversies in inguinal hernia repair. *Outpatient Surg Mag*. 2000;1(8). <http://www.outpatientsurgery.net/issues/2000/08/controversies-in-inguinal-hernia-repair>.
4. Neumayer I, Giobbie-Hurder A, Jonasson O, Fitzgibbons R, Dunlop D, Gibbs J, Reda D, Henderson W. Open mesh versus laparoscopic mesh repair of inguinal hernia. *N Engl J Med*. 2004; 350:1819–7.
5. Cozad M., Ramshaw BR, Grant DN, Bachman SL, Grant DA, Grant SA. Materials characterization of explanted polypropylene, polyethylene terephthalate, and expanded polytetrafluoroethylene composites: spectral and thermal analysis. *J Biomed Mater Res B*. 2010;49B:455–2.
6. Costello CR, Bachman SL, Ramshaw BR, Grant SA. Materials characterization of explanted heavyweight polypropylene hernia meshes. *J Biomed Mater Res B*. 2007;83B:44–9.
7. Deeken CR, Abdo MS, Frisella MM, Matthews BD. Physico-mechanical evaluation of polypropylene, polyester, and polytetrafluoroethylene meshes for inguinal hernia repair. *J Am Coll Surg*. 2011;212(1):68–79.
8. Laurikainen EH, Valpas A, Kivela A, Kalliola T, Rinne K, Takala T, Nilsson CG. Retropubic compared with transobturator tape placement in treatment of urinary incontinence: a randomized controlled trial. *Obstet Gynecol*. 2007;109:4–11.
9. Rehder P, Glodny B, Richler R, Mitterberger MJ. Massive retropubic hematoma after minimal invasive mid-urethral sling procedure in a patient with a corona mortis. *Eur Urol*. 2008;53: 288–308.
10. U.S. Food and Drug Administration. *Urogynecologic Surgical Mesh Implants*. <http://www.fda.gov/MedicalDevices/ProductsandMedicalProcedures/ImplantsandProsthetics/UroGynSurgicalMesh/default.htm>. Accessed 1 April 2012.
11. Costello CR, Bachman SL, Cleveland DS, Loy TS, Grant SA, Ramshaw BR. Characterization of heavyweight and lightweight polypropylene prosthetic mesh explants from a single patient. *Surg Innov*. 2007;14:168–76.
12. Mihaly J, Sterkel S, Ortner H, Kocsis L, Hajba L, Furdyga E, Mink J. FTIR and FT-Raman spectroscopic study on polymer based high pressure digestion vessels. *Croat Chem Acta*. 2006;79:497–501.
13. Ratner B, Hoffman AS, Schoen FJ, Lemons JE, editors. *Biomaterials science*. London: Elsevier Academic Press; 1996. p. 243–4.
14. Bracco P, Brunella V, Trossarelli L, Coda A, Botto-Micca F. Comparison of polypropylene and polyethylene terephthalate (Dacron) meshes for abdominal wall hernia repair: a chemical and morphological study. *Hernia*. 2005;9:51–5.
15. Fayolle B, Audouin L, Verdu J. Oxidation induced embrittlement in polypropylene—a tensile testing study. *Polym Degrad Stab*. 2000;70:333–40.

16. He P, Xiao Y, Zhang P, Xing C, Zhu N, Zhu X. Thermal degradation of syndiotactic polypropylene and the influence of stereoregularity on the thermal degradation behavior by *in situ* FTIR spectroscopy. *Polym Degrad Stab.* 2005;88:473–9.
17. Lappan U, Geibler U, Lunkwitz K. Electron beam irradiation of polytetrafluoroethylene in vacuum at elevated temperature: an infrared spectroscopic study. *J Appl Polym Sci.* 1999;74:1571–6.
18. Pugmire DL, Wetteland CJ, Duncan WS, Lakis RE, Schwartz DS. Cross-linking of polytetrafluoroethylene during room-temperature irradiation. *Polym Degrad Stab.* 2009;94:1533–41.
19. Clave A, Yahi H, Hammou JC, Montanari S, Gounon P, Clave H. Polypropylene as a reinforcement in pelvic surgery is not inert: comparative analysis of 100 explants. *Int Urogynecol J.* 2010;21:261–70.
20. Waler C, Sigbritt K. Assessment of thermal and thermo-oxidative stability of multi-extruded recycled PP, HDPE and a blend thereof. *Polym Degrad Stab.* 2002;78:385–91.
21. Burger JWA, Halm JA, Wijsmuller AR, ten Raa S, Jeekel J. Evaluation of new prosthetic meshes for ventral hernia repair. *Surg Endosc Other Interv Tech.* 2006;20(8):1320–5.
22. Riepe G, Loos J, Imig H, Schroder A, Schneider E, Petermann J, Rogge A, Ludwig M, Schenke A, Nassut R, Chakfe N, Morlock M. Long-term *in vivo* alterations of polyester vascular grafts in humans. *Eur J Vasc Endovasc Surg.* 1997;13:540–8.
23. Elison BJ, Frisella MM, Matthews BD, Deeken CR. Effect of repetitive loading on the mechanical properties of synthetic hernia repair materials. *J Am Coll Surg.* 2011;213(3):430–5.
24. Hernández-Gascón B, Peña E, Melero H, Pascual G, Doblaré M, Ginebra MP, Bellón JM, Calvo B. Mechanical behavior of synthetic surgical meshes: finite element simulation of the herniated abdominal wall. *Acta Biomater.* 2011;7:3905–13.